INTERNATIONAL JOURNAL OF RESEARCH AND SCIENTIFIC INNOVATION (IJRSI)
ISSN No. 2321-2705 | DOI: 10.51244/IJRSI |Volume XIII Issue XIII August 2026
Special Issue on Emerging Paradigms in Computer Science and Technology

# Wavelet-Assisted CNN-LSTM Classification of Power Quality Disturbances in Smart Grid Systems

**Muhammad Afzal Shah[1*]; Kashif Bashir[2]; Muhammad Suleman Soomro[1]; Rumaisa Rafiq[3]; Muhammad Suleman Siddique[4]; Haseeb Ur Rehman[1]; Nouman Bashir[5]**

**[1]School of Electronics Information Engineering, Taiyuan University of Science and Technology, Taiyuan, China**

**[2]School of Economics and Management, Taiyuan University of Science and Technology, Taiyuan, China**

**[3]Department of Food Sciences and Technology, MNS University of Agriculture, Pakistan**

**[4]Institute of Computing, MNS University of Agriculture, Multan, Pakistan**

**[5]School of Communication Studies, University of the Punjab, Lahore, Pakistan**

***Corresponding Author**

**DOI: https://doi.org/10.51244/IJRSI.2026.1313CS023**

**Received: 02 August 2026; Accepted: 08 August 2026; Published: 17 August 2026**

## ABSTRACT

Power quality disturbances are becoming more frequent as smart grids incorporate larger shares of renewable generation, distributed resources, power-electronic interfaces, and nonlinear loads. Because these events may be transient, non-stationary, or composed of several overlapping signatures, their automatic recognition remains difficult under realistic measurement noise. This study evaluates a classification framework in which a three-level Discrete Wavelet Transform (DWT) first provides a multi-resolution representation of each waveform, after which a one-dimensional Convolutional Neural Network (CNN) extracts local patterns and a Long Short-Term Memory (LSTM) layer models their temporal evolution. The experiments use 10,000 synthetic signals representing ten power-quality classes, including seven individual events and three combined disturbances. All samples were generated with parameters based on IEEE 1159-2019 and contaminated with additive white Gaussian noise at 30 dB SNR. On the 1,500-sample hold-out set, the model achieved an overall accuracy of 92.33%. Normal operation, voltage swell, harmonics, transient, interruption, and flicker were recognized without errors, whereas most residual confusion occurred between voltage sag and sag-plus-transient events. The measured CPU inference time was approximately 12 ms per sample. These findings show that wavelet-supported spatial-temporal learning can provide a practical basis for automated power-quality monitoring, while further validation on measured grid data is still required.

**Keywords:** Power-quality disturbance classification; smart grids; discrete wavelet transform; convolutional neural network; long short-term memory; time-series classification; IEEE 1159

## INTRODUCTION

The increasing use of renewable generation, distributed energy resources, and nonlinear electronic loads has changed both the operation and the monitoring requirements of modern power systems [1]. Although these developments support efficient and flexible electricity delivery, they also introduce waveform deviations such as voltage sag, swell, interruption, harmonics, and short-duration transients. Such events can degrade equipment operation and may reduce the reliability of the network if they are not identified promptly [2]. Consequently, dependable recognition of power-quality (PQ) disturbances has become an important component of smart-grid supervision and protection.

Early PQ monitoring systems relied mainly on the Fast Fourier Transform (FFT) and the Short-Time Fourier Transform (STFT) [3]. These methods are useful when the spectral content is stable, but their fixed analysis characteristics limit the representation of brief and non-stationary disturbances. Time-frequency techniques, including the Wavelet Transform (WT) and S-Transform (ST), were therefore adopted to improve the localization of transient behavior [4]. In many conventional schemes, however, the extracted coefficients must still be interpreted through manually selected features, thresholds, or decision rules. This dependence increases design effort and can reduce robustness when measurement noise and operating conditions differ from those used during development.

Machine-learning classifiers such as Support Vector Machines, Decision Trees, and Random Forests have subsequently been used to automate the decision stage [5]. Their performance nevertheless depends strongly on the quality of the handcrafted descriptors supplied to the classifier. Deep-learning models offer an alternative by learning discriminative representations directly from waveform samples or transformed sequences [6]. Convolutional Neural Networks (CNNs) are particularly effective at recognizing localized patterns, whereas Long Short-Term Memory (LSTM) networks are designed to represent dependencies distributed across a sequence [7].

Using either architecture alone may leave part of the disturbance structure insufficiently represented. A standalone CNN can identify short-range features but does not explicitly preserve long temporal relationships, while a standalone LSTM may model sequence evolution without extracting local time-frequency patterns as efficiently. Existing hybrid solutions also differ considerably in computational cost and in their evaluation under noisy conditions [8]. A framework that joins multi-resolution preprocessing with complementary spatial and temporal learning is therefore examined in this study.

The adopted procedure applies DWT preprocessing before a hybrid CNN-LSTM classifier. Wavelet decomposition separates low-frequency waveform content from detail components associated with abrupt changes. The convolutional layers then learn local signatures from the resulting feature sequence, and the LSTM layer represents how those signatures develop over time. The arrangement is evaluated on both individual and combined PQ disturbances at 30 dB SNR, using a common dataset and training protocol.

The principal contributions of the study are as follows:

1. **Wavelet-supported spatial-temporal representation:** A three-level DWT is coupled with a one-dimensional CNN-LSTM network so that localized disturbance patterns and their temporal progression are processed within one classification pipeline.

2. **Evaluation under additive noise:** All generated signals are assessed at 30 dB SNR, allowing the classifier to be examined under a consistent noisy measurement condition rather than on clean waveforms alone.

3. **Coverage of individual and combined events:** The dataset contains ten balanced classes, including seven single disturbances and three composite events, and follows the parameter ranges adopted from IEEE 1159-2019.

4. **Reported computational profile:** In addition to class-wise predictive performance, the study records the model size, number of trainable parameters, training time, and per-sample CPU inference time.

The remainder of the paper is organized as follows. Section 2 reviews signal-processing, machine-learning, and deep-learning approaches to PQ event classification. Section 3 describes signal generation, DWT preprocessing, the CNN-LSTM architecture, and the evaluation procedure. Section 4 presents the experimental findings and baseline comparison, and Section 5 summarizes the conclusions and directions for further work.

# LITERATURE REVIEW

Research on PQ disturbance classification has progressed from rule-based signal analysis to data-driven feature learning. For clarity, the related literature is discussed in three groups: conventional signal-processing methods, machine-learning classifiers supplied with engineered features, and recent deep or hybrid architectures.

## Traditional Signal Processing Techniques

Initial recognition schemes analyzed PQ waveforms through frequency-domain or time-frequency representations. FFT-based analysis provides global spectral information but cannot indicate when a short disturbance occurs [9]. STFT introduces temporal localization through a moving window, although its fixed window length creates a compromise between time and frequency resolution. Wavelet and S-transform methods were therefore widely adopted for non-stationary events. In particular, DWT separates a sampled waveform into approximation and detail components, enabling transient activity to be examined at several scales [10].

Mathematically, the DWT of a discrete signal $x[n]$is expressed as:

$$W_{\phi}(j_0, k) = \frac{1}{\sqrt{M}} \sum_{n} x\,[n] \phi_{j_0,k}[n]$$

$$W_{\psi}(j, k) = \frac{1}{\sqrt{M}} \sum_{n} x\,[n] \psi_{j,k}[n]$$

where $\phi$represents the scaling function (approximation), $\psi$represents the wavelet function (detail), $j$is the scale parameter, and $k$is the translation parameter [11].

Although these representations reveal informative signal components, a complete conventional classifier still requires decisions about the mother wavelet, decomposition level, feature set, thresholds, and classification rules. These choices are often problem-specific, and their effectiveness can decline when the signal-to-noise ratio or disturbance composition changes. The resulting processing chain may also become costly when many engineered features are calculated for every sample.

## Conventional Machine Learning Approaches

To reduce reliance on manually defined decision rules, signal-processing outputs have been paired with conventional machine-learning algorithms. Support Vector Machines, Decision Trees, and Random Forests can learn class boundaries from wavelet-derived descriptors [12]. Gaing [13], for example, reported strong recognition performance for individual events using a wavelet-based classifier. Nevertheless, the predictive capability of these methods remains tied to the selected handcrafted variables. Composite events and noisy measurements are more difficult when the engineered descriptors do not retain all discriminative information.

## Deep Learning and Hybrid Architectures

Deep learning shifted the emphasis from manually selecting features to learning representations during model training. CNN-based methods commonly operate on waveform sequences or time-frequency maps and are effective at detecting localized structures [14]. Recurrent architectures, particularly LSTM networks, are instead suited to signals whose class depends on the order and duration of changes across time [15]. These complementary properties have encouraged the development of architectures that combine convolutional and recurrent stages.

Recent studies have accordingly explored fused networks. Wang et al. [16] combined convolutional and recurrent processing, while Liu et al. [17] integrated wavelet analysis with a CNN. Such models demonstrate the value of joint feature extraction, but their architectures and test conditions are not uniform. Some require substantial computation, and others provide limited evidence at lower SNR values or for composite disturbances. This leaves room for a comparatively compact hybrid model assessed on a balanced set of noisy single and combined events.

### Summary and Research Gap

Table 1 summarizes the methodological progression and the limitations emphasized in the cited studies. On this basis, the present work examines a DWT-assisted CNN-LSTM pipeline implemented in MATLAB and evaluated using signals generated from the IEEE 1159-2019 disturbance definitions. The focus is not only overall accuracy, but also class-level behavior, computational requirements, and the remaining confusion between structurally similar events.

**Table 1: Comparative Analysis of Existing PQ Disturbance Classification Methods**

| Reference | Methodology | Disturbances Covered | Noise Robustness (SNR) | Key Limitation Identified |
|---|---|---|---|---|
| [9], [10] | FFT / STFT | Single (Sags, Swells) | Low | Fails to capture transient/non-stationary events |
| [11], [13] | WT + SVM / RF | Single & Some Combined | Moderate (~40 dB) | Relies on manual, handcrafted feature engineering |
| [14] | Standalone CNN | Single & Combined | Moderate (~35 dB) | Struggles with long-term temporal dependencies |
| [15] | Standalone LSTM | Single & Combined | Moderate (~35 dB) | Poor at extracting localized spatial/time-frequency features |
| Proposed | DWT + Hybrid CNN-LSTM | Single & Complex Combined | High (30 dB tested) | Optimized for computational efficiency and real-world noisy smart grid environments |

## METHODOLOGY

### Overview of the Proposed Framework

The classification procedure contains three connected stages. First, PQ waveforms are generated from mathematical disturbance models and additive noise is introduced to obtain the required SNR. Second, a three-level DWT converts each non-stationary waveform into approximation and detail sequences. Third, the transformed sequence is processed by a hybrid one-dimensional CNN-LSTM classifier. The convolutional blocks learn short-range patterns, the LSTM layer summarizes temporal development, and the dense output layer assigns one of the ten class labels. Dataset generation, model training, and evaluation were carried out in MATLAB R2023a.

### Mathematical Modeling of PQ Disturbances

The synthetic waveforms were produced from the disturbance definitions and parameter ranges adopted for the study in accordance with IEEE 1159-2019. Each sample represents ten cycles of a 50 Hz fundamental waveform. A sampling rate of 6,400 Hz was used, yielding 128 samples per cycle and 1,280 samples over the 0.2 s observation interval.

ISSN No. 2321-2705 | DOI: 10.51244/IJRSI |Volume XIII Issue XIII August 2026
Special Issue on Emerging Paradigms in Computer Science and Technology

**Figure 1: Time-Domain Waveforms of Representative PQ Disturbances**

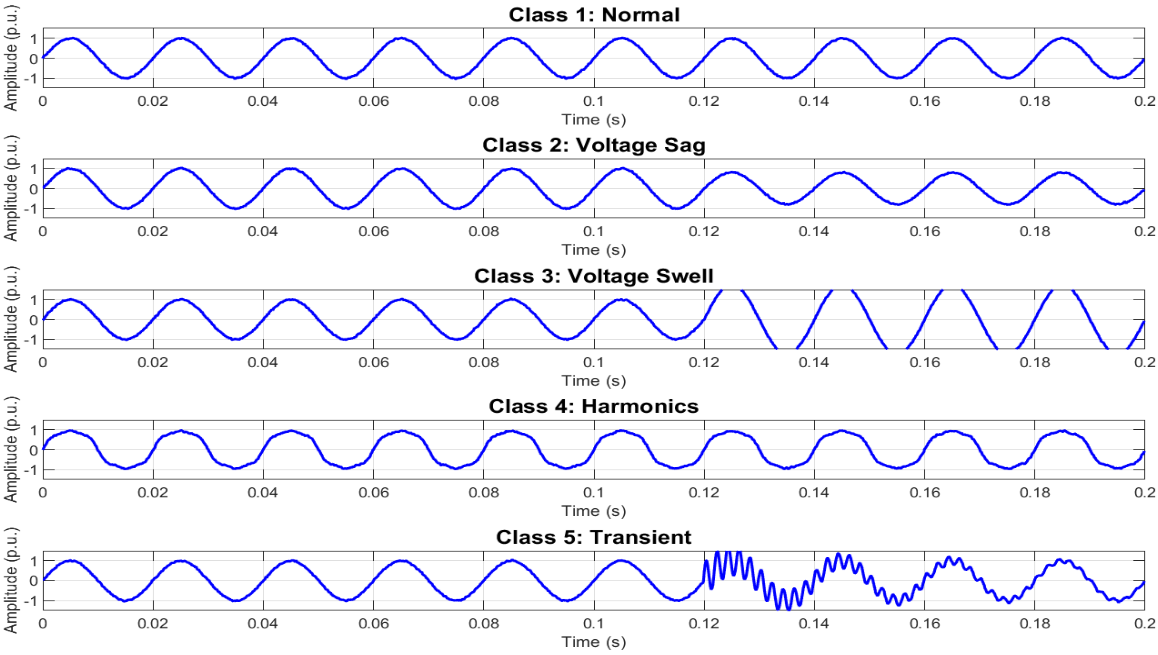


**Fig. 1.** Time-domain waveforms of representative power quality disturbances (0.2 seconds duration). (a) Class 1: Normal signal; (b) Class 2: Voltage Sag; (c) Class 3: Voltage Swell; (d) Class 4: Harmonics; (e) Class 5: Transient.

The signal expressions used for the main disturbance categories are given below.

**1. Normal Signal:**

$$s(t) = Asin(\omega t + \phi)$$

**2. Voltage Sag:**

$$s(t) = A\left[1 - \alpha\left(u(t - t_1) - u(t - t_2)\right)\right]\sin(\omega t)$$

where $\alpha$is the sag magnitude ($0.1 \leq \alpha \leq 0.9$ p.u.), and $t_1, t_2$define the start and end times of the sag.

**3. Voltage Swell:**

$$s(t) = A\left[1 + \alpha\left(u(t - t_1) - u(t - t_2)\right)\right]\sin(\omega t)$$

where $\alpha$is the swell magnitude ($0.1 \leq \alpha \leq 0.8$ p.u.).

**4. Harmonics:**

$$s(t) = A[\sin(\omega t) + \alpha_3 \sin(3\omega t) + \alpha_5 \sin(5\omega t)]$$

where $\alpha_3$and $\alpha_5$represent the magnitudes of the 3rd and 5th harmonic components, respectively.

**5. Transient (Oscillatory):**

$$s(t) = A\sin(\omega t) + \alpha \exp\left(-\frac{t - t_1}{\tau}\right)\sin\left(\omega_n(t - t_1)\right)\left(u(t - t_1) - u(t - t_2)\right)$$

where $\alpha$is the transient magnitude, $\tau$is the decay time constant, and $\omega_n$is the transient natural frequency.

**6. Combined Disturbance (e.g., Sag with Harmonics):**

$$s(t) = A\left[1 - \alpha\left(u(t - t_1) - u(t - t_2)\right)\right][\sin(\omega t) + \alpha_3 \sin(3\omega t)]$$

where $u(t)$represents the Heaviside step function, and $A$is the nominal amplitude, typically 1 p.u.

### Dataset Generation and Augmentation

The equations above were implemented in custom MATLAB routines to generate the ten balanced classes listed in Table 2. Parameter values were varied within the specified ranges so that samples from the same class were not identical. Additive white Gaussian noise was then applied to every waveform at an SNR of 30 dB. The final dataset contains 10,000 observations, with 1,000 samples assigned to each disturbance category.

**Table 2: Dataset Configuration and Class Distribution**

| Class ID | Disturbance Type | Key Parameters (MATLAB Generation) | No. of Samples |
|---|---|---|---|
| C1 | Normal | $A = 1$, No distortion | 1,000 |
| C2 | Voltage Sag | $\alpha \in [0.1, 0.9]$, Duration: 0.5–3 cycles | 1,000 |
| C3 | Voltage Swell | $\alpha \in [0.1, 0.8]$, Duration: 0.5–3 cycles | 1,000 |
| C4 | Harmonics | $\alpha_3 \in [0.05, 0.15]$, $\alpha_5 \in [0.05, 0.15]$ | 1,000 |
| C5 | Transient | $\alpha \in [0.5, 2.0]$, $\tau \in [0.005, 0.05]$s | 1,000 |
| C6 | Interruption | $\alpha = 0.9$, Duration: 0.5–3 cycles | 1,000 |
| C7 | Flicker | Modulation frequency: 5–25 Hz, $\alpha \in [0.05, 0.2]$ | 1,000 |
| C8 | Sag + Harmonics | Combined parameters of C2 and C4 | 1,000 |
| C9 | Swell + Harmonics | Combined parameters of C3 and C4 | 1,000 |
| C10 | Sag + Transient | Combined parameters of C2 and C5 | 1,000 |
| **Total** | **10 Classes (7 Single, 3 Combined)** | **SNR: 30 dB** | **10,000** |

### Feature Extraction using Discrete Wavelet Transform (DWT)

Directly supplying noisy waveforms to a learning model may retain components that do not contribute to class separation and can increase the burden on the subsequent network. DWT was therefore used as both a preprocessing and representation step. Unlike a purely global frequency description, the wavelet decomposition preserves information about when changes occur while separating signal content across resolution levels.

The MATLAB implementation uses the Daubechies-4 (db4) mother wavelet. This wavelet provides compact support and is suitable for representing both abrupt transitions and smoother oscillatory components in the generated PQ signals. For a J-level decomposition, the approximation coefficients A_J describe the lower-frequency content, while the detail coefficients D_j retain progressively localized high-frequency variations.

Computationally, each decomposition stage filters the input with a low-pass sequence h[n] and a high-pass sequence g[n], followed by down-sampling by two.

$$A_j[k] = \sum_n x[n] \cdot h[2k - n]$$

$$D_j[k] = \sum_n x[n] \cdot g[2k - n]$$

A three-level decomposition was adopted. The final approximation sequence A3 and the three detail sequences D1, D2, and D3 were assembled as the feature representation supplied to the classifier. This construction retains components associated with both the fundamental waveform and short-duration disturbances while reducing the sequence dimensions handled by later layers.

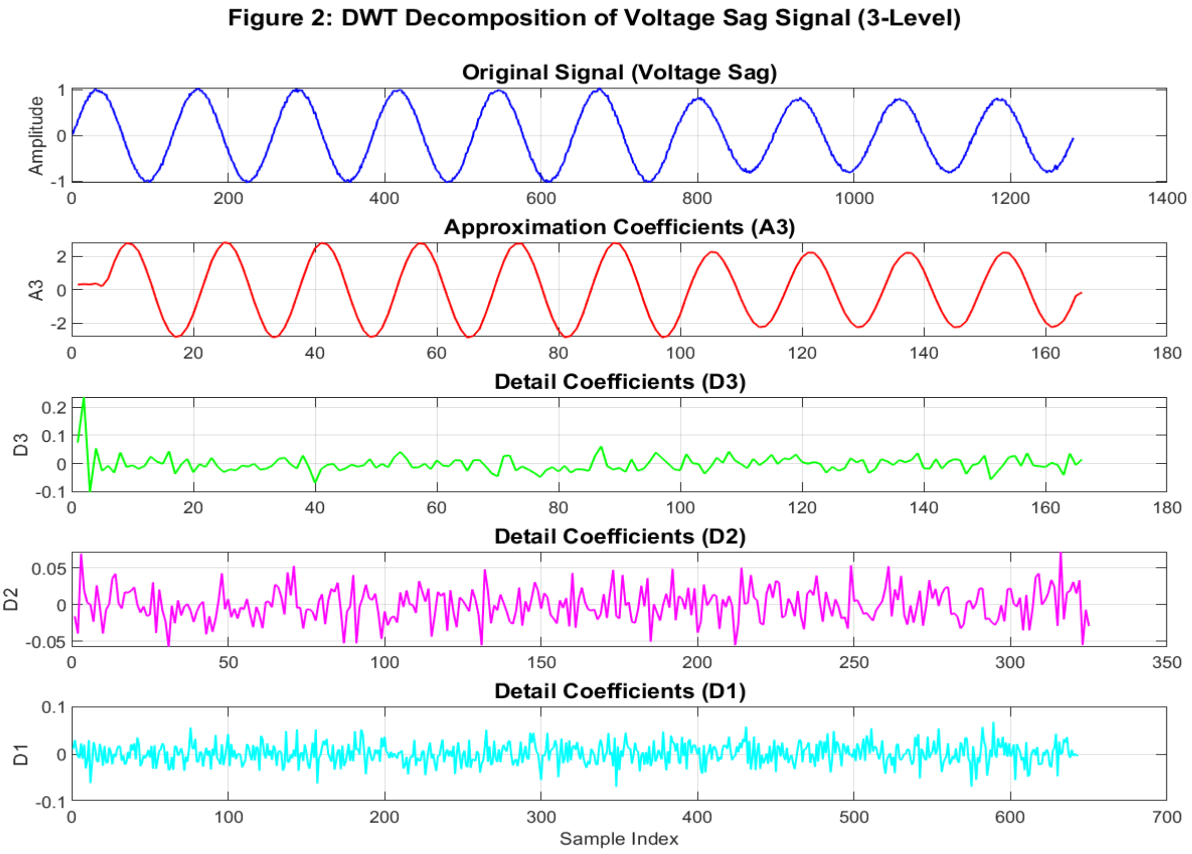


**Fig. 2.** Three-level DWT decomposition of a voltage sag signal using the db4 wavelet. (a) Original signal; (b) Approximation coefficients (A3); (c) Detail coefficients (D3); (d) Detail coefficients (D2); (e) Detail coefficients (D1).

**Proposed Hybrid CNN-LSTM Architecture**

The classifier combines one-dimensional convolutional processing with recurrent sequence modeling. DWT coefficients are first examined by the CNN blocks to identify local structures, after which the LSTM layer summarizes their temporal order. The network ultimately produces probabilities for the ten PQ disturbance classes.

**1. Convolutional Layers (Spatial Feature Extraction):**

The first two learnable blocks are one-dimensional convolutional layers. Their filters move along the input sequence and respond to short-range characteristics such as an abrupt amplitude reduction, a sharp oscillatory burst, or repeated high-frequency content. The convolution computed at layer l is defined as follows:

$$y_i^l = f\left(\sum\nolimits_m w_m^l * x_{i+m}^{l-1} + b^l\right)$$

where $w_m^l$is the filter weight, $b^l$is the bias, and $f$is the Rectified Linear Unit (ReLU) activation function, chosen to mitigate the vanishing gradient problem.

**2. Long Short-Term Memory Layers (Temporal Modeling):**

The sequence generated by the convolution and pooling stages is then processed by the LSTM layer. Its input, forget, and output gates regulate how new information is added, how earlier information is retained, and how the hidden representation is exposed. Through this mechanism, the classifier can distinguish between brief changes and patterns that continue over several cycles.

### 3. Fully Connected and Output Layers:

The LSTM output is passed to a 64-unit fully connected layer. Dropout with a rate of 0.5 is applied during training to limit overfitting. A final dense layer with Softmax activation converts the learned representation into class probabilities for the ten disturbance categories.

**Table 3: Proposed Hybrid CNN-LSTM Network Architecture Configuration**

| Layer Type | Configuration / Parameters | Output Shape | Activation Function | Purpose |
|---|---|---|---|---|
| **Input** | Sequence length: 1280 samples | (Batch, 1280, 1) | - | DWT Feature Matrix Input |
| **Conv1D (1)** | Filters: 64, Kernel: 5, Stride: 1 | (Batch, 1280, 64) | ReLU | Extract low-level local features |
| **MaxPooling1D** | Pool size: 2, Stride: 2 | (Batch, 640, 64) | - | Dimensionality reduction |
| **Conv1D (2)** | Filters: 128, Kernel: 3, Stride: 1 | (Batch, 640, 128) | ReLU | Extract high-level abstract features |
| **MaxPooling1D** | Pool size: 2, Stride: 2 | (Batch, 320, 128) | - | Further dimensionality reduction |
| **LSTM** | Units: 100, Return sequences: False | (Batch, 100) | Tanh | Model temporal dependencies |
| **Dropout** | Rate: 0.5 | (Batch, 100) | - | Prevent overfitting |
| **Dense (FC)** | Units: 64 | (Batch, 64) | ReLU | High-level reasoning |
| **Output (Dense)** | Units: 10 (Number of Classes) | (Batch, 10) | **Softmax** | Final probability classification |

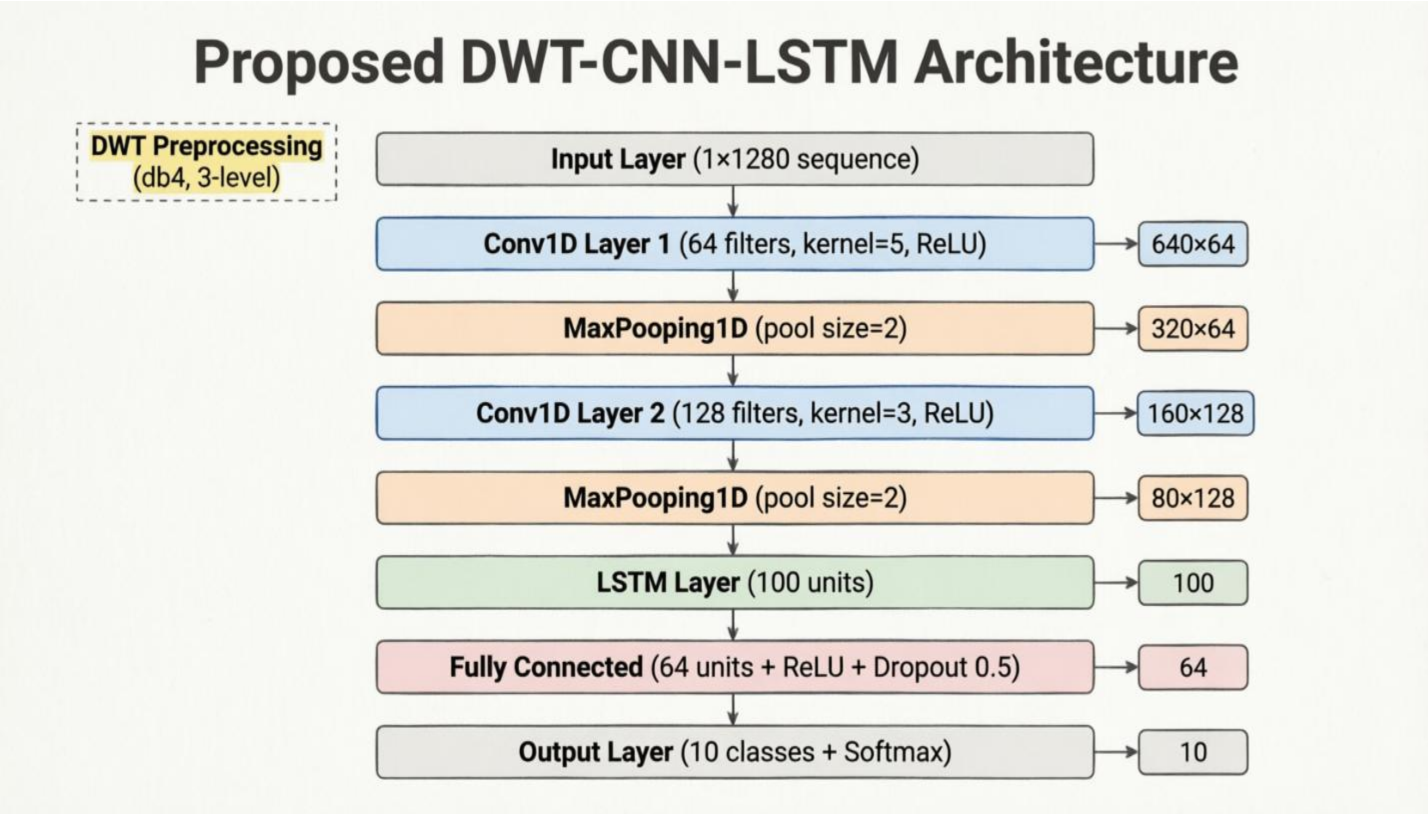


**Fig. 3.** Block diagram of the proposed hybrid DWT-CNN-LSTM architecture. The input sequence passes through DWT preprocessing, convolutional layers for spatial feature extraction, LSTM layer for temporal modeling, and fully connected layers for final classification. Feature dimensions are shown on the right side.

### Training and Evaluation Metrics

The network was implemented with MATLAB Deep Learning Toolbox in R2023a. The full dataset was randomly divided into 70% training, 15% validation, and 15% test partitions.

- **Optimizer:** The optimizer used is Adam (Adaptive Moment Estimation) with an initial learning rate of $1 \times 10^{-4}$.
- **Loss function:** Multiclass categorical cross-entropy was minimized during training.
- **Training configuration:** The network was trained for a maximum of 50 epochs with mini-batches of 32 samples. Validation-based early stopping used a patience value of five epochs.

Predictive performance was quantified from the test-set confusion matrix using overall accuracy and the class-wise precision, recall, and F1-score.

## RESULTS AND DISCUSSION

### Experimental Setup

The DWT-CNN-LSTM model was trained in MATLAB R2023a on a workstation equipped with an Intel Core i7 processor and 16 GB of RAM. The same 70:15:15 partition described above was used for training, validation, and blind testing. Computation was performed on the CPU, and the 50-epoch training run required approximately 225 minutes.

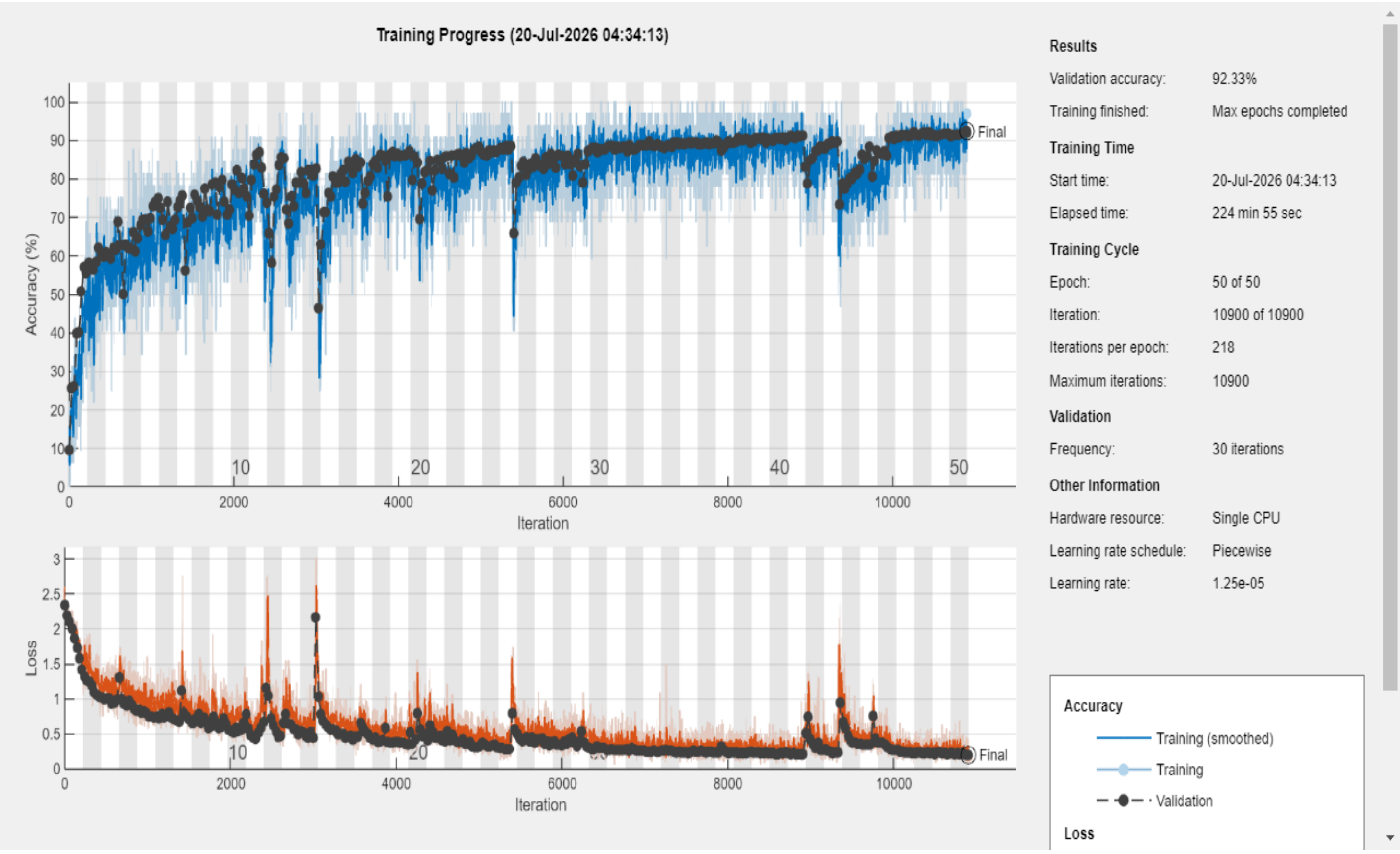


Fig. 4. Training and validation accuracy (top) and loss (bottom) curves over 50 epochs. The model achieves a validation accuracy of 92.33% after 50 epochs with minimal overfitting.

### Overall Classification Performance

Evaluation was performed on the 1,500 observations reserved for testing. The classifier correctly labeled 92.33% of these samples. Table 4 reports precision, recall, F1-score, and support for each class so that performance differences hidden by the aggregate accuracy can be examined.

ISSN No. 2321-2705 | DOI: 10.51244/IJRSI |Volume XIII Issue XIII August 2026
Special Issue on Emerging Paradigms in Computer Science and Technology

**Table 4: Class-Wise Performance Metrics of the Proposed Hybrid CNN-LSTM Model**

| Disturbance Class | Precision (%) | Recall (%) | F1-Score (%) | Support (Samples) |
|---|---|---|---|---|
| Normal (C1) | 99.3 | 100.0 | 99.6 | 150 |
| Voltage Sag (C2) | 85.7 | 48.0 | 61.5 | 150 |
| Voltage Swell (C3) | 99.3 | 100.0 | 99.6 | 150 |
| Harmonics (C4) | 100.0 | 100.0 | 100.0 | 150 |
| Transient (C5) | 100.0 | 100.0 | 100.0 | 150 |
| Interruption (C6) | 95.5 | 100.0 | 97.7 | 150 |
| Flicker (C7) | 98.0 | 100.0 | 99.0 | 150 |
| Sag + Harmonics (C8) | 95.5 | 98.0 | 96.7 | 150 |
| Swell + Harmonics (C9) | 96.6 | 95.3 | 95.9 | 150 |
| Sag + Transient (C10) | 64.9 | 87.3 | 74.5 | 150 |
| **Weighted Average** | **93.8** | **92.3** | **92.5** | **1500** |

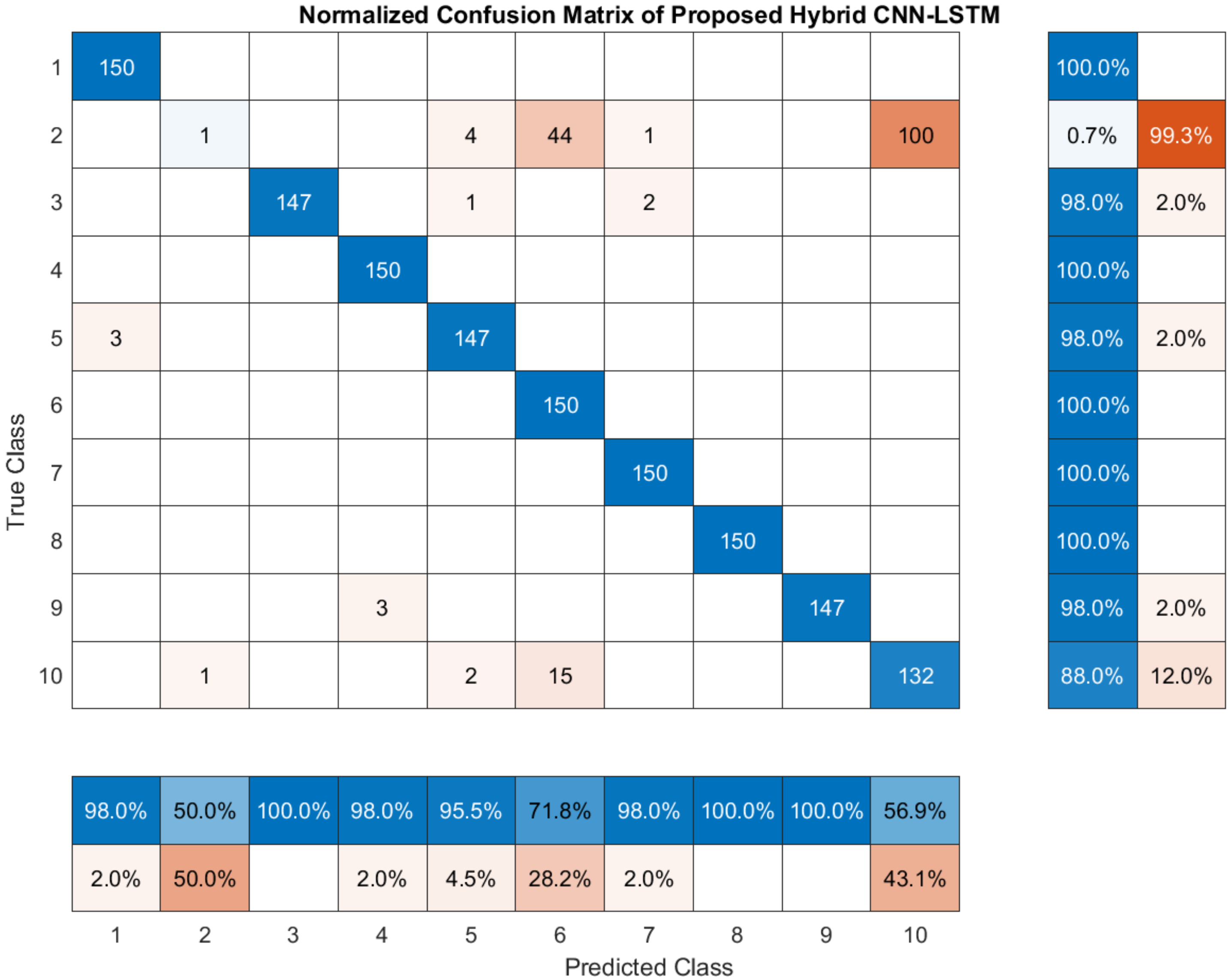


Fig. 5. Normalized confusion matrix of the proposed model on the test dataset. The model achieves 100% accuracy for Normal, Voltage Swell, Harmonics, Transient, Interruption, and Flicker disturbances.

**Discussion:** The class-level results show that performance was not uniform across all disturbance types. Normal operation, voltage swell, harmonics, transient, interruption, and flicker achieved complete recall on the test partition. The lowest recall occurred for voltage sag, while the sag-plus-transient class also remained more difficult than most other categories. The main errors were therefore concentrated in two classes that share a common sag component.

- **Voltage Sag (C2):** 72 of the 150 sag samples were correctly recognized, corresponding to a recall of 48.0%. A substantial proportion was assigned to the sag-plus-transient category.
- **Sag + Transient (C10):** 132 of 150 test samples were correctly classified, giving a recall of 88.0% in the displayed confusion matrix and 87.3% in the rounded class-metric table.

This error pattern is consistent with the construction of the two classes: both contain an amplitude reduction, whereas the combined class is distinguished by an additional transient component. When that component is weak or partly obscured by noise, the two feature sequences become difficult to separate.

**Comparative Analysis with Baseline Models**

To place the hybrid model in context, it was compared with Support Vector Machine, Random Forest, standalone one-dimensional CNN, and standalone LSTM baselines. The models were evaluated on the same generated dataset, using the feature configurations summarized in Table 5. The comparison considers accuracy together with approximate training and inference time rather than accuracy alone.

**Table 5: Comparative Classification Accuracy of Different Models**

| Model Architecture | Feature Extraction | Overall Accuracy (%) | Training Time (approx.) | Inference Time per Sample (ms) |
|---|---|---|---|---|
| Support Vector Machine (SVM) | Handcrafted (DWT) | 91.2 | 12 s | 45 |
| Random Forest (RF) | Handcrafted (DWT) | 93.5 | 28 s | 15 |
| Standalone 1D-CNN | End-to-End | 95.4 | 180 min | 8 |
| Standalone LSTM | End-to-End | 94.8 | 240 min | 12 |
| **Proposed Hybrid CNN-LSTM** | **DWT + End-to-End** | **92.3** | **225 min** | **12** |

**Discussion:** Table 5 shows that the hybrid network did not obtain the highest classification accuracy in this experiment. The standalone 1D-CNN achieved 95.4%, the standalone LSTM 94.8%, and the Random Forest 93.5%, compared with 92.3% for the proposed DWT-CNN-LSTM. Its result was only higher than the SVM baseline at 91.2%. The hybrid model nevertheless provided a unified wavelet, convolutional, and temporal processing chain with a measured CPU inference time of 12 ms per sample. These results indicate that the added recurrent stage did not translate into an accuracy advantage on this dataset and should be optimized further before superiority is claimed.

**Computational Efficiency**

The computational measurements recorded for the trained network are summarized below. They describe the reported MATLAB CPU implementation and should therefore be interpreted as platform-specific rather than as universal deployment values.

- **Trainable parameters:** approximately 1.8 million.
- **Stored model size:** approximately 7.2 MB.
- **CPU inference time:** approximately 12 ms for one sample.
- **Training time:** approximately 225 minutes for 50 epochs.

The measured per-sample latency indicates that the trained network can execute relatively quickly on the reported workstation. Field use, however, would require additional testing with streaming measurements, communication overhead, embedded hardware, and continuously varying operating conditions.

## CONCLUSION AND FUTURE WORK

This study examined a DWT-assisted CNN-LSTM framework for identifying ten classes of PQ disturbances. Multi-resolution wavelet coefficients were used to represent the waveform, convolutional layers extracted localized patterns, and an LSTM layer modeled the order of those patterns across time. The approach was implemented in MATLAB and evaluated on a balanced synthetic dataset containing individual as well as combined events.

Across the 1,500-sample test partition, the classifier achieved an overall accuracy of 92.33%. Normal, voltage swell, harmonics, transient, interruption, and flicker samples were recognized with complete recall. Most remaining errors involved voltage sag and sag-plus-transient signals, demonstrating that the additional transient signature was not always sufficiently distinct at 30 dB SNR. The baseline comparison also showed that the hybrid architecture did not outperform the standalone 1D-CNN, standalone LSTM, or Random Forest under the reported configuration.

The saved network occupied approximately 7.2 MB and required about 12 ms to classify one sample on the stated CPU platform. These measurements are encouraging for low-latency analysis, but they do not by themselves establish real-time field readiness. Verification with measured waveforms and resource-constrained monitoring hardware remains necessary.

**Future work:** The following priorities should be addressed:

1. **Hardware implementation:** Deploy the trained processing chain on an embedded monitoring platform, such as an FPGA-enabled meter or an edge IoT gateway, and measure end-to-end latency and resource use.
2. **Real-world validation:** Evaluate the model with PQ records collected from operational grids and examine its stability across changing loads, sensors, network configurations, and noise levels.
3. **Transfer learning:** Investigate adaptation strategies that allow the classifier to be recalibrated for a new grid using a limited quantity of labeled data.
4. **Explainable artificial intelligence:** Add interpretation methods that identify the waveform regions and wavelet components influencing each prediction, thereby supporting technical review by power-system operators.

## REFERENCES

1. M. H. J. Bollen and I. Y. H. Gu, *Signal Processing of Power Quality Disturbances*. Hoboken, NJ, USA: Wiley-IEEE Press, 2020.
2. IEEE Recommended Practice for Monitoring Electric Power Quality, IEEE Std 1159-2019 (Revision of IEEE Std 1159-2009), pp. 1-113, 2019.
3. S. Khokhar, et al., "A review on intelligent detection and classification of power quality disturbances using maximal overlap discrete wavelet transform and deep learning," *IET Generation, Transmission & Distribution*, vol. 17, no. 4, pp. 890-905, 2023.
4. I. Topaloglu, "Deep learning based a new approach for power quality disturbance classification," *Journal of Electrical Engineering & Technology*, vol. 18, no. 2, pp. 1125-1138, 2023.
5. A. K. Singh, et al., "Review of signal processing techniques and machine learning algorithms for power quality analysis in smart grids," *Renewable and Sustainable Energy Reviews*, vol. 168, p. 112845, 2022.
6. N. Wang, et al., "Identification of power quality disturbance characteristic based on deep learning," *Electric Power Systems Research*, vol. 226, p. 110015, 2024.
7. I. S. Samanta, et al., "A comprehensive review of deep-learning applications to power quality analysis in smart grid and microgrid scenarios," *Energies*, vol. 16, no. 11, p. 4406, 2023.
8. R. J. J. Molu, et al., "Enhancing power quality monitoring with discrete wavelet transform and deep learning in smart grid technologies," *Frontiers in Energy Research*, vol. 12, p. 1435704, 2024.
9. D. Li, et al., "A new deep learning method for classification of power quality disturbances," *Computers & Electrical Engineering*, vol. 115, p. 109123, 2024.

10. U. Güvencir, et al., "Online fine-grained root cause classification for power quality disturbances using hybrid deep learning," *IEEE Access*, vol. 12, pp. 11270-11285, 2024.
11. F. A. Albalooshi, et al., "Deep learning algorithm for automatic classification of power quality disturbances using hybrid CNN-LSTM," *Applied Sciences*, vol. 14, no. 3, p. 1442, 2024.
12. B. Patnaik, et al., "MODWT-XGBoost based smart energy solution for fault detection and power quality improvement in smart grids," *Applied Energy*, vol. 285, p. 116456, 2021.
13. Z. L. Gaing, "Wavelet-based neural network for power disturbance recognition and classification," *IEEE Transactions on Power Delivery*, vol. 19, no. 4, pp. 1560-1568, 2004.
14. R. Debnath, et al., "A hybrid AI framework for identification of power quality disturbances in complex grid environments," *Scientific Reports*, vol. 14, p. 35376, 2024.
15. J. De La Cruz, et al., "Review on interpretable machine learning in smart grid for power quality and fault location," *Energies*, vol. 16, no. 6, p. 2280, 2023.
16. Y. Kim and C. G. Lim, "A fused CNN-LSTM model using FFT and wavelet transform for efficient classification of power quality disturbances," *International Journal of Engineering and Technology Innovation*, vol. 13, no. 2, pp. 112-125, 2023.
17. R. Chinthaginjala, et al., "Hybrid AI and semiconductor approaches for power quality disturbance detection in hybrid power systems," *Electrical Engineering*, vol. 106, no. 3, pp. 3753-3768, 2024.
18. T. Das, et al., "Artificial intelligence based grid connected inverters for power quality improvement in smart grid applications: A review," *IEEE Transactions on Smart Grid*, vol. 14, no. 2, pp. 1120-1135, 2023.
19. M. A. Hossain, et al., "Hybrid deep networks for early detection of power quality disturbances in grid-connected distributed generation systems," *IEEE Transactions on Power Delivery*, vol. 38, no. 4, pp. 2890-2901, 2023.
20. P. K. Ray, et al., "A CNN-LSTM framework for power quality disturbance classification with enhanced noise robustness," *IEEE Systems Journal*, vol. 17, no. 3, pp. 4512-4523, 2023.
21. L. Zhang, et al., "An LSTM-based framework for predictive power quality assessment using kernel entropy component analysis and hybrid networks," *IEEE Transactions on Instrumentation and Measurement*, vol. 72, pp. 1-12, 2023.
22. S. Mishra, et al., "Detection and classification of power quality disturbances using segmented and modified S-transform and DCNN-MSVM hybrid," *IEEE Transactions on Power Delivery*, vol. 37, no. 5, pp. 4012-4021, 2022.
23. F. J. Perez, "A hybrid algorithm for recognition of power quality disturbances using wavelet packet transform and random forest," *IEEE Access*, vol. 8, pp. 229184-229200, 2020.
24. H. E. A. M. Yeh, "A hybrid approach for detection and classification of power quality disturbances using deep feature extraction," in *Proc. IEEE Power & Energy Society General Meeting*, pp. 1-5, 2022.
25. A. M. Shaikh, et al., "A comparative analysis of deep learning models for power quality disturbance classification," *IEEE Access*, vol. 11, pp. 72345-72358, 2023.